CHAPTER III

Gold-Based Bulk Metallic Glass

Abstract

Gold-based bulk metallic glass alloys based on Au-Cu-Si are introduced. The alloys have a gold content comparable to 18-karat gold. They show a very low liquidus temperature below 700 K, a large supercooled liquid region, and good processibility. The maximum casting thickness exceeds 5 mm in the best glass former. This $Au_{49}Ag_{5.5}Pd_{2.3}Cu_{26.9}Si_{16.3}$ *alloy has a liquidus temperature of 644 K, a glass transition temperature of 401 K, and a supercooled liquid region of 58 K. The Vickers hardness of these alloys is ~350 Hv, twice that of typical conventional 18-karat crystalline gold alloys. The Au-based BMG alloy families were studied and characterized for GFA-determination parameters, atomic size effect, oxygen contamination, and elastic constants. The results were compared with published models and previous findings on other BMG alloys, and show that Au-based BMG is a unique alloy family with closest resemblance to the Pt-based BMG family.*

1. Introduction

Gold became known to mankind thousands of years ago and has been of inestimable value to civilization ever since. It is the noblest of noble metals, and has a good combination of high thermal conductivity, high electrical conductivity, and high corrosion resistance. These properties have resulted in extensive use of gold and its alloys in electronics, aerospace, astronomy, medical, and industrial applications. However, gold has always been most valued as a jewelry material. Gold alloys are easy to fashion, are non-allergenic, have a bright pleasing color, and remain tarnish free indefinitely. Pure gold and higher karat gold alloys, however, are rather soft and thereby vulnerable to wear and scratching. This results in diminished aesthetic appearance and is a drawback of conventional crystalline gold alloys.

In the last two decades, several alloys based on Pd [1-3], La [4], Zr [5, 6], Fe [7-9], and Pt [10] were found to form bulk amorphous phases during relatively slow cooling. Fully amorphous samples are obtained when the alloys are cast into copper molds of a diameter up to centimeters. This indicates critical cooling rates for glass formation of 100 K/s or less. Bulk metallic glasses (BMGs) exhibit properties such as high strength, large elastic strain limit, and in some rare but desirable cases, substantial ductility [11]. The compositions of these BMGs are typically close to a deep eutectic composition. Consequently, their melting temperatures are much lower than estimated from interpolation of the alloy constituents' melting temperatures. The resulting low liquidus temperature is an attractive property for casting alloys. The extraordinary stability of BMG-forming alloys against crystallization also results in a large supercooled liquid

region, ΔT, ($\Delta T=T_x-T_g$, T_x is crystallization temperature, Tg is glass transition temperature), the temperature region in which the amorphous phase first relaxes to a highly viscous liquid before eventually crystallizing. In this temperature region BMGs are amenable to thermoplastic processing using net-shape processing methods similar to those employed for thermoplastics or conventional glass blowing [12].

2. Background and Motivation

The binary gold silicon eutectic composition was the first alloy found to exhibit metallic glass formation by Duwez and co-workers in 1960 [13]. The critical cooling rate for glass formation of this alloy is on the order of 10^6 K/s, resulting in a critical casting thickness, d_c, below 50 microns. By partially substituting Si by Ge, an increase in both the glass forming ability and the width of the supercooled liquid region were observed [14, 15]. The poor glass forming ability of these early metallic glasses and the low glass transition temperature make these alloys of only marginal interest for most applications and explains the limited interest in these metallic glasses over the past several decades.

2.1 Scientific Motivation

A high Poisson's ratio seems to be the key to plasticity in metallic glasses (reader is referred to Chapter IV, Section 1-2). Prior to the author's Au-based BMGs discovery [16] there were only two families of BMGs that exhibited an exceptionally high Poisson's ratio (above 0.4). These were the BMG systems based on palladium (~0.41)

and platinum (~0.43) [11], both of which showed exceptional ductility. In the periodic table there are only three pure elements that have Poisson's ratios higher than 0.4 – 0.45 for Tl, 0.44 for Pb, and 0.44 for Au. Because of the toxicity and health problems found in Tl and Pb, Au-based BMG seemed to be the ideal alloy candidate for investigating the relationship between plasticity and Poisson's ratio.

2.2 Commercial Motivation[A] and Key Objectives

A suitable amorphous gold based alloy suitable for most applications (e.g., jewelry) requires a T_g of at least 370 K to be stable at ambient temperatures. Other desirable properties include: a large gold content (~18 karat or higher), high hardness, good processibility, and a critical casting thickness that permits fabrication of net-shaped articles such as jewelry. From a processing point of view, it is desirable to have a large supercooled liquid region which gives access to a low forming viscosity, which in turn enables thermoplastic processing.

3. Fundamental Study of Gold Bulk Metallic Glass

3.1 Experimental

Samples were prepared by alloying the elements (Au: 99.95%, Cu: 99.9%, Ag: 99.5%, Pd: 99.95%, Si: 99.95% purity) in an arc-melter. Copper mold quenching was

[A] Commercial and industrial interests seem to generate the best financial support.

performed to solidify the alloy in its amorphous state, and to determine the critical casting thickness. Thermal analysis was performed in a differential scanning calorimeter (DSC) Netzsch DSC 404c. X-ray diffraction (XRD) was carried out on an Inel XRG 3000 using Cu Kα radiation. Hardness tests were performed on a Leco R-600.

3.2 Results and Discussion

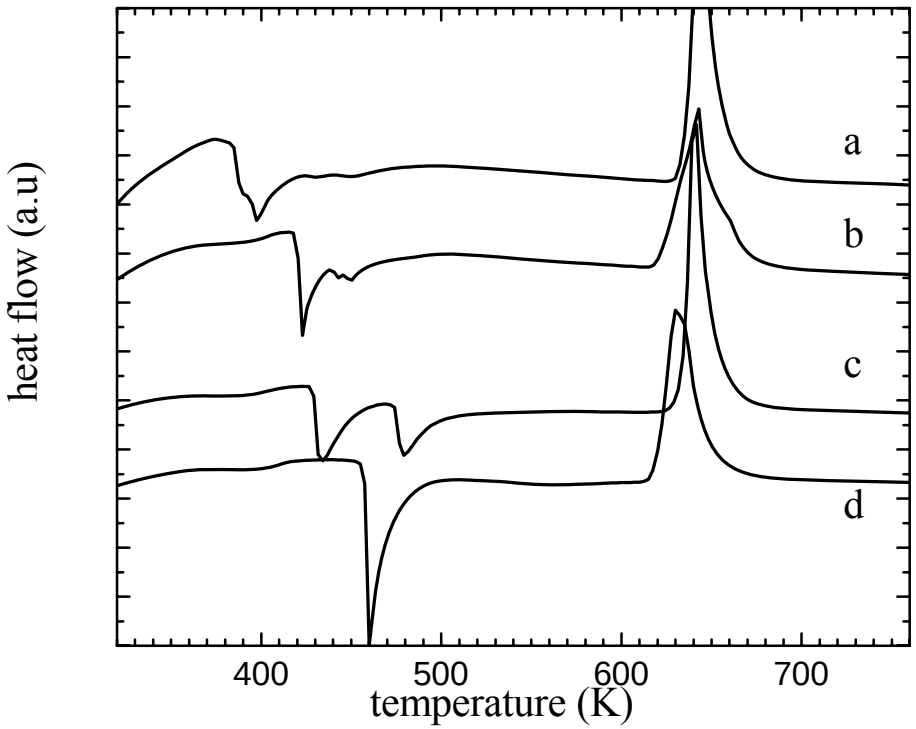

Figure III-1: DSC thermogram determined by heating with 20 K/min of gold-based alloys of various compositions that were cast in copper molds of various sizes

a: $Au_{55}Cu_{25}Si_{20}$ cast in 0.5 mm copper mold

b: $Au_{46}Ag_5Cu_{29}Si_{20}$ cast in 1 mm copper mold

c: $Au_{52}Pd_{2.3}Cu_{29.2}Si_{16.5}$ cast in 2 mm copper mold

d: $Au_{49}Ag_{5.5}Pd_{2.3}Cu_{26.9}Si_{16.3}$ cast in 5 mm copper mold

Figure III-1 shows the DSC thermograms obtained by heating at a rate of 20 K/min for four gold alloys. The thermogram in Figure III-1a is that of $Au_{55}Cu_{25}Si_{20}$ which was cast in a 0.5 mm copper mold. Figure III-1b shows $Au_{46}Ag_5Cu_{29}Si_{20}$ cast at 1 mm. Figure III-1c shows $Au_{52}Pd_{2.3}Cu_{29.2}Si_{16.5}$ cast at 2 mm. And Figure III-1d shows $Au_{49}Ag_{5.5}Pd_{2.3}Cu_{26.9}Si_{16.3}$ cast at 5 mm. All compositions are in atomic percent. All alloys show a glass transition and a crystallization peak suggesting that at least some fraction of the material was amorphous. A comparison of the heat of crystallization (ΔH) and the heat of fusion (H_f), which are summarized for the various alloys in Table III-1, gives approximately $\Delta H/H_f = 0.6$, a value typical for an entirely amorphous sample. When comparing with the T_g of the early gold alloys of about 300 K [13-15] all alloys have surprisingly high T_g. Their T_g is higher than 370 K, with the exception of $Au_{55}Cu_{25}Si_{20}$, thereby exceeding requirements for most jewelry applications.

Composition [at.%]	Tg [K]	Tx [K]	ΔT [K]	Tl [K]	Trg =Tg/Tl	d_c [mm]	ΔH [J/g]	H_f [J/g]
$Au_{49}Ag_{5.5}Pd_{2.3}Cu_{26.9}Si_{16.3}$	401	459	58	644	0.62	5	35	46
$Au_{52}Pd_{2.3}Cu_{29.2}Si_{16.5}$	393	427	34	651	0.60	2	33	49
$Au_{46}Ag_5Cu_{29}Si_{20}$	395	420	25	664	0.59	1	28	46
$Au_{55}Cu_{25}Si_{20}$	348	383	35	654	0.53	0.5	32	57

Table III-1: Summary of the properties of the various gold-based alloys. The maximum thickness at which the alloy could be cast amorphous, d_c, was determined by copper mold quenching into strip geometry.

Figure III-2 shows the x-ray diffractogram of the four alloys. The diffractogram in Figure III-2a is that of $Au_{55}Cu_{25}Si_{20}$ cast in a 0.5 mm copper mold. Figure III-2b shows

$Au_{56}Ag_5Cu_{29}Si_{20}$ cast at 1 mm. Figure III-2c shows $Au_{52}Pd_{2.3}Cu_{29.2}Si_{16.5}$ cast at 2 mm, and Figure III-2d shows $Au_{49}Ag_{5.5}Pd_{2.3}Cu_{26.9}Si_{16.3}$ cast at 5 mm. All spectra show a broad maxima typical for entirely amorphous material, supporting the DSC results.

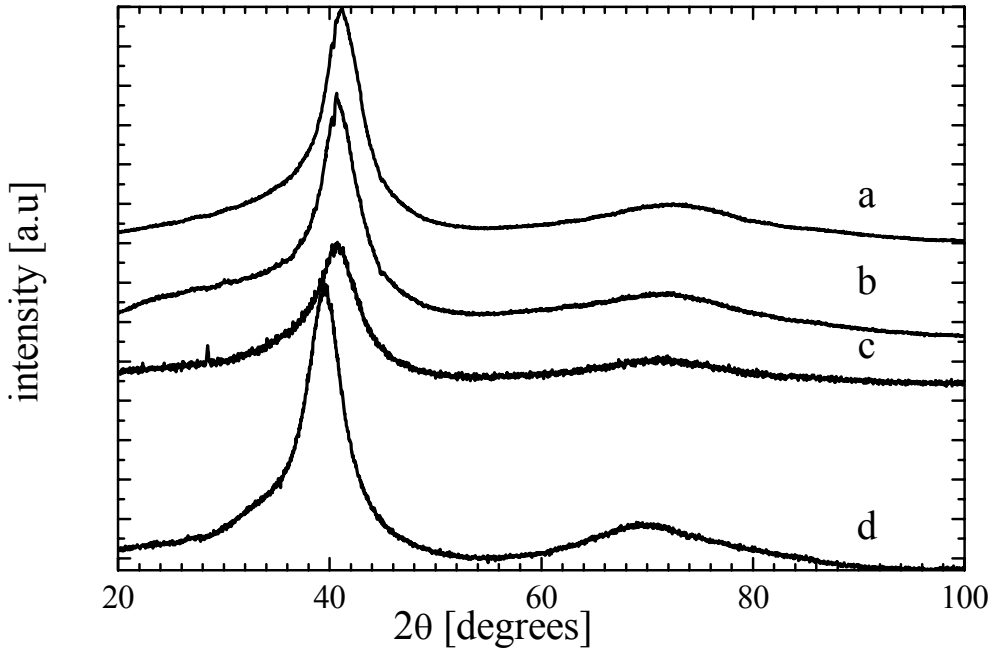

Figure III-2: X-ray diffraction thermogram of gold based alloys of various compositions that were cast in copper molds with various diameters

a: $Au_{55}Cu_{25}Si_{20}$ cast in 0.5 mm copper mold

b: $Au_{46}Ag_5Cu_{29}Si_{20}$ cast in 1 mm copper mold

c: $Au_{52}Pd_{2.3}Cu_{29.2}Si_{16.5}$ cast in 2 mm copper mold

d: $Au_{49}Ag_{5.5}Pd_{2.3}Cu_{26.9}Si_{16.3}$ cast in 5 mm copper mold

The results are summarized in Table III-1. All alloys show liquidus temperatures of below 700 K. Specifically, $Au_{49}Ag_{5.5}Pd_{2.3}Cu_{26.9}Si_{16.3}$ has a liquidus temperature as low as 644 K. With the glass transition temperature of 401 K, the alloy has the reduced glass

transition temperature, Trg (=T_g/T_l), of 0.62, a value only seen among good bulk metallic glass formers [17]. The supercooled liquid region for $Au_{55}Cu_{25}Si_{20}$, $Au_{56}Ag_5Cu_{29}Si_{20}$, and $Au_{52}Pd_{2.3}Cu_{29.2}Si_{16.5}$ is approximately 30 K. For $Au_{49}Ag_{5.5}Pd_{2.3}Cu_{26.9}Si_{16.3}$, the supercooled liquid region is 58 K.

3.3 Validity of ΔT and Trg Parameters

Δ*T,* (= Tx – Tg), is often used as a parameter that describes the formability of a BMG [7, 18, 19]. The ΔT parameter represents the width of the supercooled liquid region. During the constant heating experiment in the DSC, the BMG solid is heated and entered into the supercooled liquid region at Tg where the glass relaxes. If the supercooled liquid has good stability against crystallization, there will be a large temperature window upon heating before the first crystallization event takes place, resulting in large ΔT. Therefore the ΔT parameter is viewed as the alloy's stability against crystallization, which implies its good GFA [20].

A larger composition range for all four alloys was studied to determine the variation of glass forming ability and ΔT with composition. As an example, during the development of $Au_{49}Ag_{5.5}Pd_{2.3}Cu_{26.9}Si_{16.3}$ alloy, the Au content was varied between 40% and 60%, Ag content was varied from 0-20%, Pd from 0-5%, Cu from 0-35 %, and Si from 14-20% (all atomic percent). Among the constituents of these alloys, the Si and Pd content have the strongest influence on the glass forming ability and ΔT. This is illustrated in Figure III-3 and Figure III-4, which show the dependence of the critical casting thickness and ΔT on Si and Pd content. The Si content was varied between 14 and

20%, resulting in a variation of d_c from 1 mm to 5 mm, and a variation of ΔT from 35 K to 60 K. By varying the Pd content from 0% to 5%, ΔT increases continuously with some scatter whereas d_c reaches a maximum at Pd = 2.3%. In both cases, a strong dependence of ΔT and d_c on the composition variations can be observed. However, no obvious correlation between ΔT and d_c – previously reported to be positive [21, 22] or negative [23, 24] – was observed. Our finding is similar to the observations [25] made by Xu et al., who discovered bulk glass former in the binary Cu-Zr alloy system. The best glass former, up to 2 mm casting thickness, was located at $Cu_{64}Zr_{36}$. There is no obvious correlation with ΔT nor Trg where nearby compositions are compared, as shown in Figure III-5.

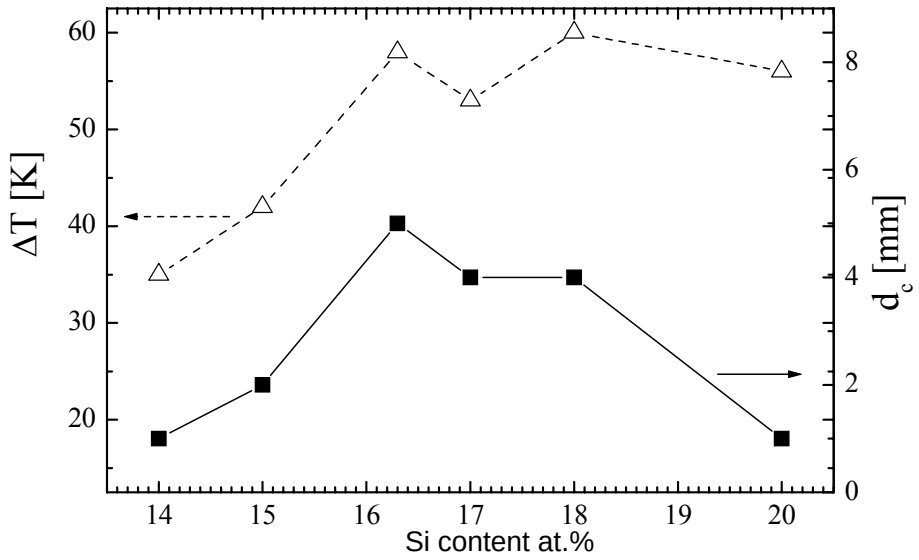

Figure III-3: Composition dependence of ΔT and d_c for $(Au_{58.5}Ag_{6.6}Pd_{2.8}Cu_{32.1})_{86-x}Si_{14+x}$ for x = 0-6%. A strong dependence on the Si content of both d_c and ΔT is observed. No obvious correlation of d_c and ΔT is seen.

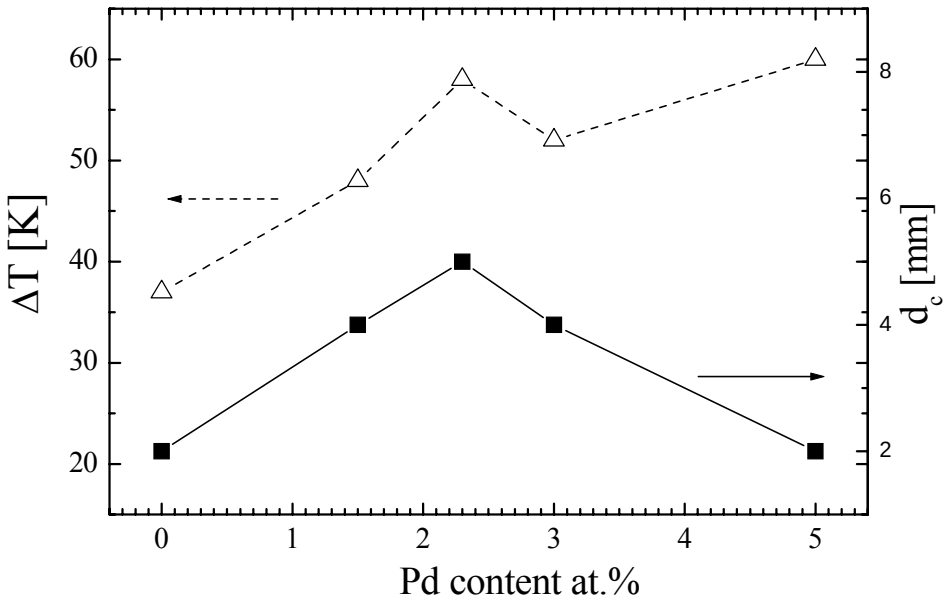

Figure III-4: Composition dependence of ΔT and d_c for $(Au_{60.1}Ag_{6.8}Cu_{33.1})_{83.7-y}Pd_ySi_{16.3}$ for y = 0-5%. A strong dependence on the Pd content of both d_c and ΔT is observed. No obvious correlation of d_c and ΔT is seen.

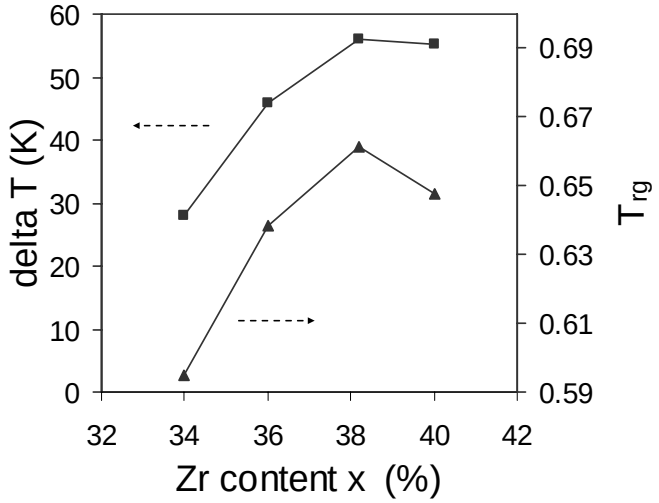

Figure III-5: Composition dependence of ΔT and Trg for $Cu_{100-X}Zr_X$ for X = 34-40%. The best glass former is located at X=36%(reproduced after [25]).

3.4 Validity of Atomic Size Ratio Using Topological Model

A topological model, based on the atomic packing and lattice topography, was suggested by Miracle [26] who realized the distinct "fingerprints" in the fraction atomic radii vs. concentration plots in many BMG systems. The reader is referred to Chapter II Section 2.2 and [26], [27], and [28] for more details. A particular example is shown in Figure III-7 for Ca-based BMGs. The size fraction decreases from 1.0 (main constituent) to 0.8, to 0.7, and then to 0.6.

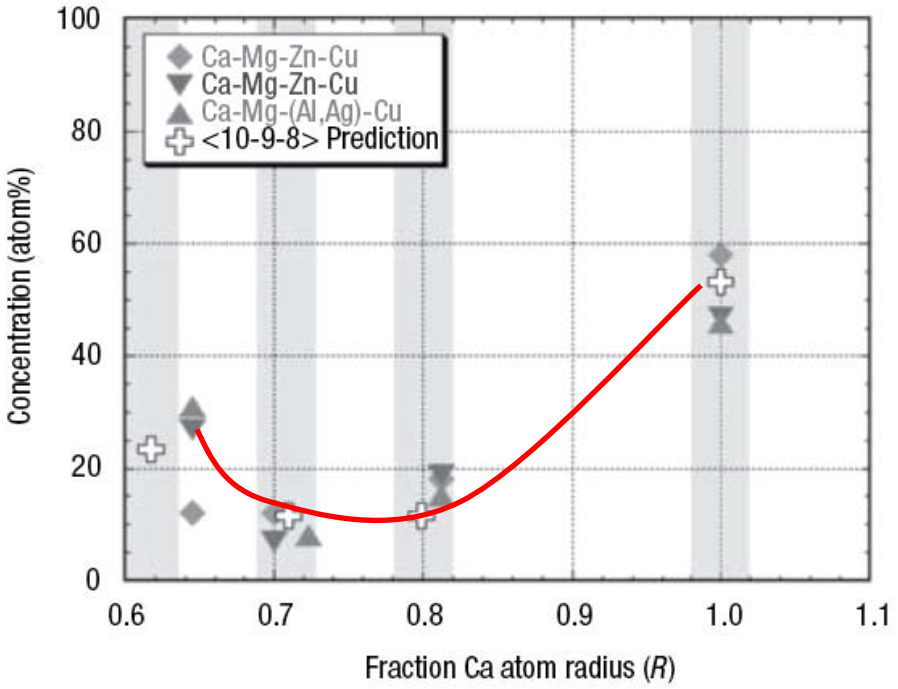

Figure III-6: Comparison of relative atomic size and concentrations for Ca-based BMGs. A distinct "fingerprint" could be seen as guided by solid curve line (after [26]).

Using the same approach, we plot the relationship between atomic radii fractions for all three high Poisson's ratio BMGs: Pd-based, Pt-based, and Au-based BMGs. A

striking similarity is found in their fingerprints. The atomic size fractions are approximately 1.0, 0.9, and 0.7 as shown in Figure III-7. The solid curve line represents an approximate trend. There is a noticeable scattering of concentrations of 0.9-radii constituents. However, the 1.0-0.9-0.7 radii fraction trend is clear, which suggests that these high Poisson's ratio BMGs could have topographically similar atomic structures.

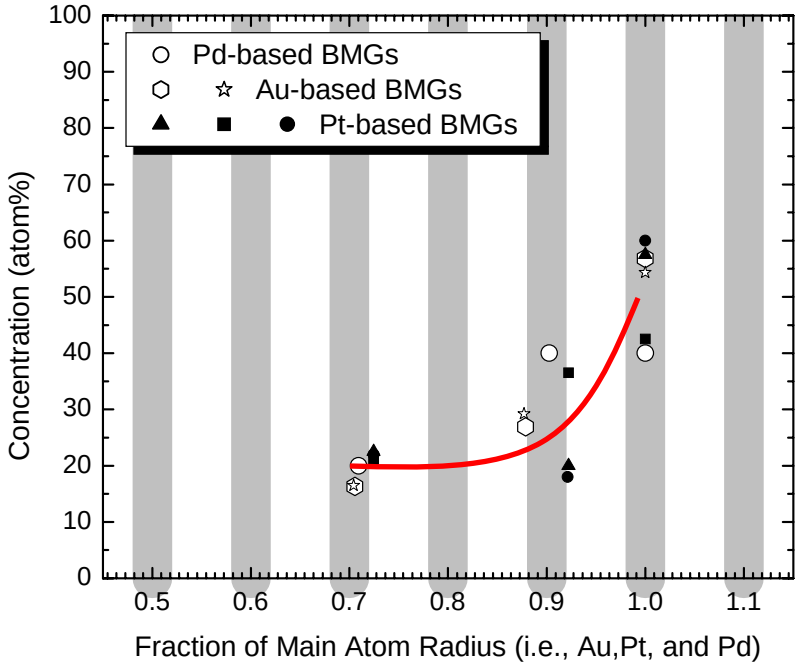

Figure III-7: Comparison of relative atomic size and concentrations for high Poisson's ratio BMGs. A distinct "fingerprint" can be seen as guided by the solid curve.

4. Elastic Constants Study

4.1 Experimental

Cast strips of Au-based BMG alloys of various compositions were synthesized by using the copper casting method. The original alloy ingots were prepared by alloying the

elements (Au: 99.95%, Cu: 99.9%, Ag: 99.5%, Pd: 99.95%, Si: 99.95%, Be: 99.5%, Mn: 99.95% Purity) in an arc-melter. The samples were then cut and polished to achieve parallel surfaces on opposite sides of the specimen. The shear and longitudinal wave speeds were measured using the pulse-echo overlap technique with 25 MHz piezoelectric transducers for each of the cast samples. Poisson's ratio (υ), Shear Modulus (G), Young's Modulus (E) and Bulk Modulus (B) were calculated from the two modes of sound velocity and the Au-BMG density of 13.72 g/cc. The alloy compositions were varied slightly from the best glass former ($Au_{49}Ag_{5.5}Pd_{2.3}Cu_{26.9}Si_{16.3}$). For example the Au content was varied while other elements were kept at relatively the same ratios. Ag, Pd, Cu, and Si were also modified slightly. Other foreign elements, e.g., Mn, Pt, and Be, were also introduced into the alloy up to 5% to check the effect of alloying elements.

4.2 Results and Discussion

Figure III-8 shows one example of many investigated correlations between compositions and υ, G, and B. Similar to the majority of the correlations tested, the plot does not reveal any trend in the change of υ versus the change in Au content. However, the plot indicates that the lowest υ value corresponds to the best glass former υ = 0.406 for $Au_{49}Ag_{5.5}Pd_{2.3}Cu_{26.9}Si_{16.3,}$ as pointed by the arrow in Figure III-9.

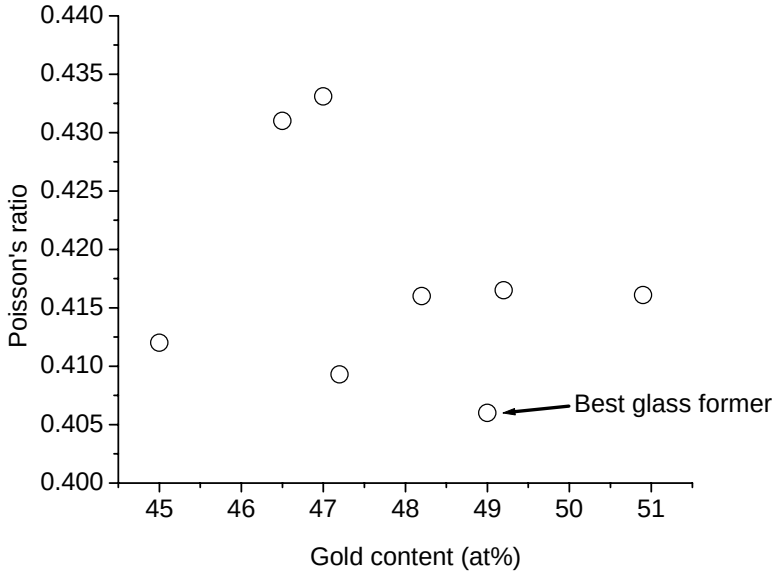

Figure III-8: Au content in the original $Au_{49}Ag_{5.5}Pd_{2.3}Cu_{26.9}Si_{16.3}$ was altered slightly to check the correlation between Au content and υ. There is no clear trend in this case. However, the best glass former is the alloy with lowest υ, as indicated in the plot.

The following compositional modifications were investigated around the original composition ($Au_{49}Ag_{5.5}Pd_{2.3}Cu_{26.9}Si_{16.3}$), but we did not observe any clear correlations between the compositions and υ, G, B:

- Be addition up to 5%
- Mn addition up to 5%
- Ag varying content 3-6%
- Pd varying content 0-2.3%

The only two trends that we observed are demonstrated in Figure III-9 and III-10 – the relationships between Cu content on G and υ are shown in Figure III-9, and Au content on G and υ are shown in Figure III-10.

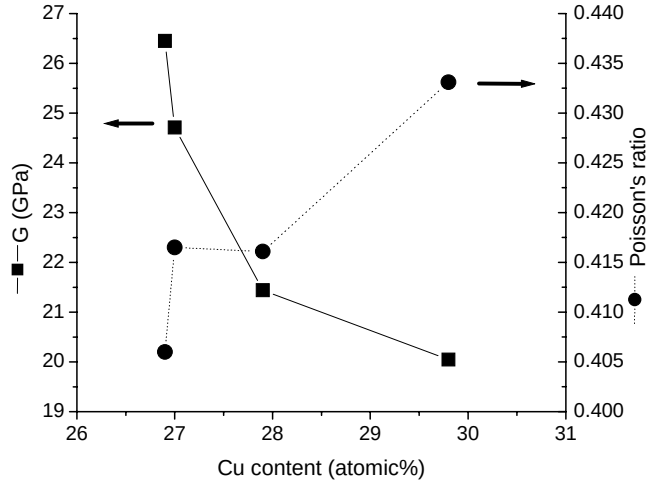

Figure III-9: Cu content in the original $Au_{49}Ag_{5.5}Pd_{2.3}Cu_{26.9}Si_{16.3}$ was altered slightly to check its correlation with G and υ. G drops as Cu content increases from the original 26.9% in the best glass former. υ is the lowest for the best glass former, but the increase in υ with respect to Cu content is not systematic.

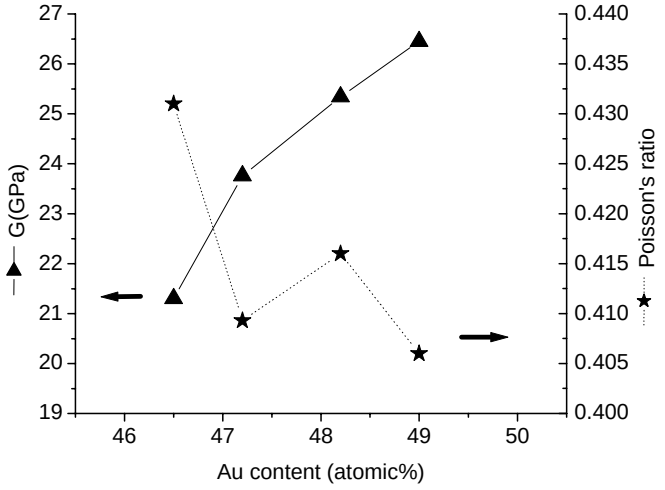

Figure III-10: Au content in the Be-bearing gold BMGs $(Au_{49}Ag_{5.5}Pd_{2.3}Cu_{26.9}Si_{16.3})_{95}Be_5$ was altered slightly to check its correlation with G and υ. G increases as Au content increases towards the original 49% in the best glass former. υ is the lowest for the best glass former, and it tends to increase as Au content is reduced.

During recent years there have been many efforts to understand the relationship between elastic constants and liquid characteristics, e.g., vitrification, structural relaxation [29], liquid fragility, and the liquid's deviation from Arrhenius behavior[30]. Many debates [30-37] have arisen out of the attempt to associate the B/G ratio, which is directly related to υ, with the deviation from Arrhenius behavior, which is quantified as the "steepness index" or "m fragility" [32]. The discrepancies in data collection associated with different viscosity measurement methods remain problematic, especially where "steepness index" is taken as the slope of the Arrhenius plot [38, 39] near Tg, where relaxation effects could complicate the data interpretation.

By comparing our viscosity data and the literature values on nominal Au-Si-Ge metallic glass [40], our results agree with the observation made by Novikov and Sokolov [30]. Our findings indicate that υ (and B/G ratio) would increase as the liquid departs from Arrhenius behavior, which appears to be opposite to a correlation established by Johari [33]. In our case, the best glass forming liquid is the strongest liquid and any minute change in the composition would result in significant drop in viscosity [41]. This may also suggest that $Au_{49}Ag_{5.5}Pd_{2.3}Cu_{26.9}Si_{16.3}$ is a kinetically stabilized glass.

5. Oxygen Impurity Study

The alloy's resistance to oxidation was studied by comparing two $Au_{49}Ag_{5.5}Pd_{2.3}Cu_{26.9}Si_{16.3}$ alloys: one alloy processed in air and the other in a vacuum of 10^{-3} mbar. Both alloys were cast in 4 mm copper molds after being overheated in the molten state to approximately 900 K for 1 minute. No difference in the surface

appearance, the DSC thermograms, nor the x-ray spectra could be observed. We conclude that the alloy's glass forming ability and its appearance is insensitive to the presence of oxygen in the processing environment. This oxygen-inert characteristic has *not* been observed before in other bulk glass forming alloys, where oxygen content and processing environments greatly influence the GFA and mechanical properties of the alloys [1, 42-45].

6. Summary

Gold based bulk metallic glass alloys were developed with a weight content comparable to 18 karat gold. The alloys show a low liquidus temperature, large supercooled liquid region, large maximum casting thickness, and good processibility for both casting and thermo-plastic processing. The combination of these properties together with good hardness (Hv=360) and esthetic appearance make them ideal for jewelry, dental, medical, and electronic applications. The summary of alloy characteristics and mechanical properties are summarized in Table III-2. A jewelry article made by thermoplastic stamping is shown in Figure III-11. The BMG is first cast into 5 mm fully amorphous strip, and then the cast strip is cut into smaller feedstock material. The feedstock meterial is then heated to 170 ºC which is 40 ºC above its glass transition temperature. Once the temperature is reached, the alloy is stamped into a mold.

Parameters for determining GFA were investigated. Atomic size ratios for these Au-BMGs were also compared topologically, and we observed a similarity among the three high Poisson's ratio glasses based on Pd, Pt, and Au. Elastic constants (υ, G, and B)

were measured and compared for alloys of different compositions. The value υ is the lowest at the best glass forming composition. The study gives additional insights to the ongoing debates on plasticity in metallic glasses and its relationship to elastic moduli, especially the Poisson's ratio [30-37].

	18K Au BMG	18K crys* Au
Melting temperature	371°C (700°F)	~1000°C (1832°F)
Casting temperature	450–600°C (842–1112°F)	>1100°C (2012°F)
Glass transition temperature	130°C (266°F)	N/A
Working temperature**	135–180°C & <370° (275–356°F) & <698°	700–1000°C (1292°–1832°F)
Critical casting thickness (mm)	5	N/A
Yield strength (MPa)	1100	350
Elastic strain limit ε_{el} (%)	1.5	~0.65
Vickers hardness (Hv), as-cast	360	100–150
Density (g/cc)	13.7	15.4

Table III-2: Summary of characteristic temperatures and mechanical properties of 18 karat gold BMG and its 18 karat crystalline alloy counterpart(*). Working temperatures(**) refer to the servicing temperatures at which the jewelry alloy could be altered, resized, or repaired.

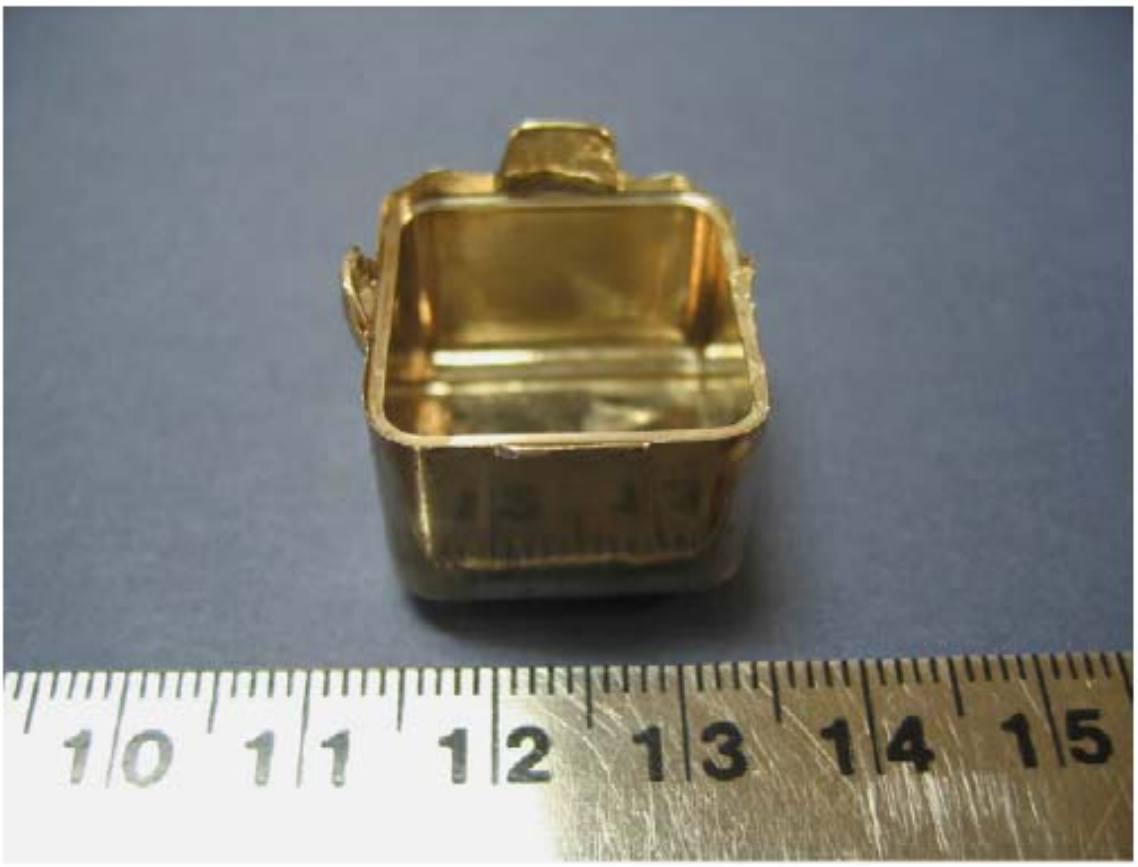

Figure III-11: A jewelry article is made by thermoplastic stamping technique.

References

[1] H. W. Kui, A. L. Greer, D. Turnbull, Applied Physics Letters 45 (1984) 615.

[2] A. Inoue, N. Nishiyama, H. Kimura, Materials Transactions Jim 38 (1997) 179.

[3] I. R. Lu, G. Wilde, G. P. Gorler, R. Willnecker, Journal of Non-Crystalline Solids 252 (1999) 577.

[4] A. Inoue, T. Nakamura, T. Sugita, T. Zhang, T. Masumoto, Materials Transactions Jim 34 (1993) 351.

[5] A. Inoue, T. Zhang, T. Masumoto, Materials Transactions Jim 31 (1990) 177.

[6] A. Peker, W. L. Johnson, Applied Physics Letters 63 (1993) 2342.

[7] V. Ponnambalam, S. J. Poon, G. J. Shiflet, Journal of Materials Research 19 (2004) 1320.

[8] V. Ponnambalam, S. J. Poon, G. J. Shiflet, V. M. Keppens, R. Taylor, G. Petculescu, Applied Physics Letters 83 (2003) 1131.

[9] Z. P. Lu, C. T. Liu, J. R. Thompson, W. D. Porter, Physical Review Letters 92 (2004).

[10] J. Schroers, W. L. Johnson, Applied Physics Letters 84 (2004) 3666.

[11] J. Schroers, W. L. Johnson, Physical Review Letters 93 (2004).

[12] B. Lohwongwatana, J. Schroers, W. L. Johnson, Hard 18K and .850 Pt Alloys That Can Be Processed Like Plastics or Blown Like Glass, in: Invited Talk, Santa Fe Symposium, Arbuquerque, NM, 2007.

[13] W. Klement, R. H. Willens, P. Duwez, Nature 187 (1960) 869.

[14] H. S. Chen, D. Turnbull, Applied Physics Letters 10 (1967) 284.

[15] H. S. Chen, D. Turnbull, Journal of Chemical Physics 48 (1968) 2560.

[16] J. Schroers, B. Lohwongwatana, W. L. Johnson, A. Peker, Applied Physics Letters 87 (2005).

[17] Z. P. Lu, H. Tan, Y. Li, S. C. Ng, Scripta Materialia 42 (2000) 667.

[18] T. Zhang, A. Inoue, Materials Transactions 44 (2003) 1143.

[19] V. Ponnambalam, S. J. Poon, G. J. Shiflet, Journal of Materials Research 19 (2004) 3046.

[20] A. Inoue, K. Kita, T. Zhang, T. Masumoto, Materials Transactions Jim 30 (1989) 722.

[21] A. Inoue, T. Zhang, T. Masumoto, Journal of Non-Crystalline Solids 156 (1993) 598.

[22] T. D. Shen, R. B. Schwarz, Applied Physics Letters 75 (1999) 49.

[23] T. A. Waniuk, J. Schroers, W. L. Johnson, Applied Physics Letters 78 (2001) 1213.

[24] Y. C. Kim, W. T. Kim, D. H. Kim, Materials Science and Engineering a-Structural Materials Properties Microstructure and Processing 375-77 (2004) 127.

[25] D. H. Xu, B. Lohwongwatana, G. Duan, W. L. Johnson, C. Garland, Acta Materialia 52 (2004) 2621.

[26] D. B. Miracle, Nature Materials 3 (2004) 697.

[27] O. N. Senkov, D. B. Miracle, Materials Research Bulletin 36 (2001) 2183.

[28] D. B. Miracle, Acta Materialia 54 (2006) 4317.

[29] M. L. Lind, G. Duan, W. L. Johnson, Physical Review Letters 97 (2006).

[30] V. N. Novikov, A. P. Sokolov, Nature 431 (2004) 961.

[31] S. N. Yannopoulos, G. P. Johari, Nature 442 (2006) E7.

[32] L. M. Wang, V. Velikov, C. A. Angell, Journal of Chemical Physics 117 (2002) 10184.

[33] G. P. Johari, Philosophical Magazine 86 (2006) 1567.

[34] V. N. Novikov, Y. Ding, A. P. Sokolov, Physical Review E 71 (2005).

[35] V. N. Novikov, A. P. Sokolov, Physical Review B 74 (2006).

[36] L. M. Wang, C. A. Angell, Journal of Chemical Physics 118 (2003) 10353.

[37] L. M. Wang, C. A. Angell, Journal of Chemical Physics 124 (2006).

[38] C. A. Angell, Science 267 (1995) 1924.

[39] A. Angell, Nature 393 (1998) 521.

[40] H. S. Chen, D. Turnbull, Journal of Metals 20 (1968) A10.

[41] B. Lohwongwatana, J. Schroers, W. L. Johnson, Physical Review Letters 96 (2006).

[42] X. H. Lin, W. L. Johnson, W. K. Rhim, Materials Transactions Jim 38 (1997) 473.

[43] Y. Yokoyama, A. Kobayashi, K. Fukaura, A. Inoue, Materials Transactions 43 (2002) 571.

[44] J. Schroers, Y. Wu, W. L. Johnson, Philosophical Magazine a-Physics of Condensed Matter Structure Defects and Mechanical Properties 82 (2002) 1207.

[45] S. Bossuyt, S. V. Madge, G. Z. Chen, A. Castellero, S. Deledda, J. Eckert, D. J. Fray, A. L. Greer, Materials Science and Engineering a-Structural Materials Properties Microstructure and Processing 375-77 (2004) 240.